Modelling Calcium Dynamics in Myelination

Kusha Sareen[1] and Anmar Khadra[1]
[1]Department of Physiology, McGill University, Montreal, Canada

Abstract

Oligodendrocytes (OLs) are CNS glial cells that insulate nerve fibers for the fast conduction of action potentials. Myelination is known to be a highly dynamic process whose underlying dynamics are currently poorly understood. Recent studies have emphasized the role of calcium as a regulator for activity-dependent myelination. This report presents a data-driven model for calcium transients in the oligodendrocyte lineage based on results from Rui et al. 2020. Time-series region-of-interest (ROI) $\Delta F/F$ calcium data in a culture of oligodendrocytes show spontaneous irregular transients depending on store-operated calcium entry. Here, we argue that these transients are stochastically-generated local travellings waves in the oligodendrocyte structure. This was done by developing a spatiotemporal computational model that incorporates calcium mobilization in and out of the cytosol, using the flux-balance equation. Our modelling efforts show the frequency of these transients increases with the inward membrane flux of calcium, explaining the observation of fast transients in the presence of high frequency neural activity. This supports a role for calcium in the maturation of the oligodendrocyte lineage, as a regulator for the growth of the actin cytoskeleton or as a transcription/translation factor for myelin basic protein (MBP). Our spatiotemporal simulations reveal that these waves annihilate upon collision and thus must have an absolute refractory period. These results thus provide insights into the mechanism regulating calcium transients in OPCs and show that they are random occurrences that do not encode information in their pattern.

1 Introduction

1.1 Motivation

Understanding neural plasticity is of paramount importance in determining how we grow and learn as a species. However, much of the progress made in the last century in understanding plasticity in the brain has been primarily "synapse-centric". In fact, much of the modern understanding is reliant on the timing of the arrival of action potentials to the post-synaptic terminal [14]. However, the role of myelin, a fatty insulating substance known to be a key determinant of nerve conduction velocity, and thus the arrival timing of action potentials, remains relatively unexplored. Evidence shows as myelinated neurons in

the CNS become more active, their myelin sheath elongates, allowing them to transmit signals more quickly. This creates a positive feedback system known as "activity-dependent myelination", where neurons that are firing more frequently have myelin sheath growth leading to greater conduction velocity and, thus, potential to fire even more frequently, as the neural network requires [1].

Calcium, a key signalling molecule in many physiological processes, has been implicated in activity-dependent myelin growth in oligodendrocytes in several studies. Indeed, calcium has been shown to be implicated in proliferation, differentiation and local protein synthesis in oligodendrocyte progenitor cells (OPCs).

1.2 The role of calcium in oligodendrocyte cell biology

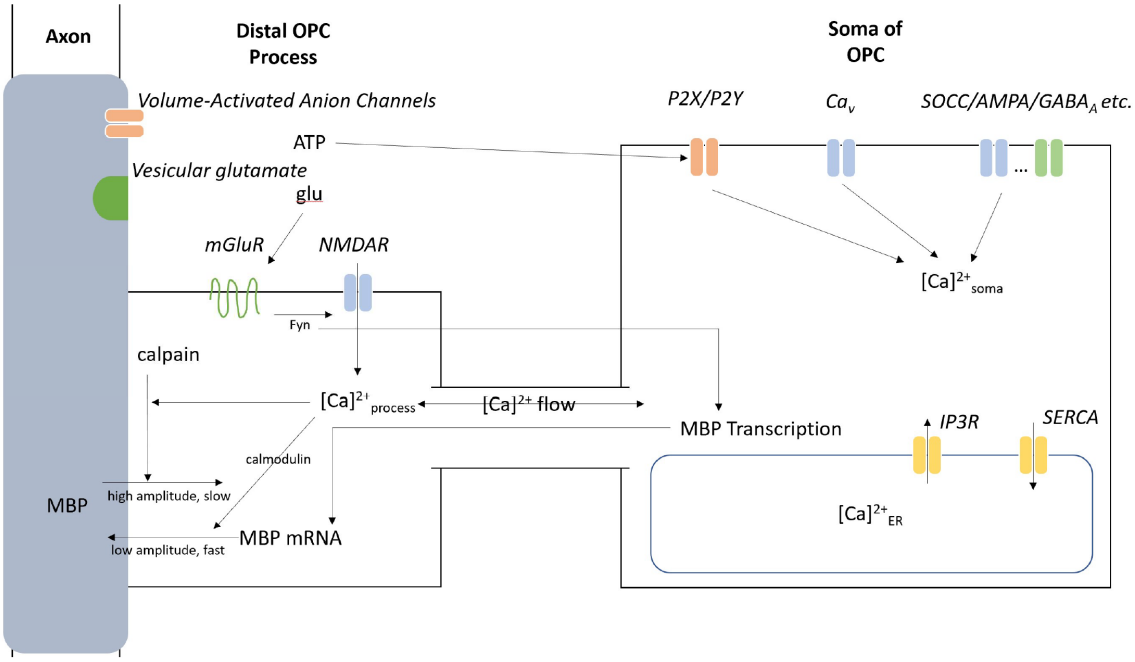

Figure 1: A schematic of the roles of different receptors and signalling molecules of the calcium dynamics of oligodendrocytes and potential implications for myelin basic protein transcription, translation and degradation.

1.2.1 Axon-dependent regulation

Axons of active nerve cells signal to local oligodendrocytes in two major ways: the release of vesicular glutamate and the release intracellular ATP through a channel [21]. ATP release occurs though a volume-regulated anion channel. This channel is activated by the osmotic swelling of an axon due to influx of ions during an action potential [6]. Additionally, vesicular release of glutamate occurs in an activity-dependent manner in both developing and mature oligodendrocytes [10]. Both ATP and glutamate thus play a role in calcium dynamics of myelinating oligodendrocytes. Variations in the release patterns of these molecules along a single axon could explain the heterogenous myelin distributions we see in the human cortex [20].

1.2.2 Signaling within oligodendrocytes

Oligodendrocytes express a number of receptors and channels governing the influx and efflux of calcium. These include voltage-gated calcium channels, AMPA-R, NMDA-R, mGluRs, GABA receptors, IP3-Rs, store-operated calcium channels (SOCCs) and purinergic receptors including P2X7 and P2Y1 [16]. It has been shown extensively that calcium currents across the membrane and somatic calcium release from the endoplasmic reticulum (ER) (through calcium-induced calcium-release mechanism) lead to transient oscillations in intracellular calcium in several different cell types [17]. In glia, it has been shown experimentally that the amplitude (maximum calcium concentration) of individual transients is positively correlated with transient duration [1]. Both in vitro and in vivo studies have further demonstrated that high-amplitude slow calcium transients lead to myelin contraction, while low-amplitude fast calcium transients lead to myelin elongation. Approximately half of the calcium transients in developing oligodendrocytes are driven by axonal action potentials, but the remaining ones occur independently of action potentials [9]. Interestingly, the frequency of calcium transients is positively correlated with speed of myelin sheath elongation. This is thought to be linked to the role of calcium in actin polymerization in the myelin sheath [1]. Additionally, it has been experimentally demonstrated that these oscillations are activity-dependent, although the underlying mechanism remains unclear. Studies have shown that sodium channel blocker TTX, blocks action potentials and, thus, decreases cal-

cium transient frequency, slowing myelin sheath growth [13]. This result thus suggests that there is a critical calcium transient frequency that marks the switch from sheath elongation to contraction. These dynamics may play a role in adult activity-dependent myelination which takes place in both motor and social learning [14].

Stretch-activated calcium channels (SACs) could also contribute to the somatic flux of calcium in oligodendrocytes. These channels are often implicated in cellular motility [21] and have been linked to mechano-electric feedback regulating calcium transients in cardiomyocytes [4]. Osmotic swelling due to the influx of calcium and other ions could translate into the activation of these mechanosensitive channels and contribute to the calcium current.

Additionally, NMDA receptors in oligodendrocytes have been linked to activity-dependent myelination. These receptors are localized at the distal processes and the myelin sheath [10]. When these receptors open, an influx of calcium results in the activation and deactivation of a number of cellular pathways localized to the sheath. The activity of these channels is controlled by glutamate-dependent mGluRs and signalling protein Fyn. Blocking vesicular glutamate release and Fyn has shown to halt myelin growth and retraction in vitro [21]. Some studies claim NMDARs are not necessary for myelination and that NMDAR-dependent signalling depends on neuregulin and BDNF which are thought to regulate their activity, expression, and trafficking, in addition to being upstream regulators of transcription factors for myelination [5] [12]. This regulation implies myelination is modulated by, but not entirely dependent on, vesicular release of glutamate in relation to coupled mGluR and NMDARs. Figure 1 depicts a summary of the role of calcium in oligodendrocyte cell biology.

1.3 Properties of spontaneous calcium transients

To understand these calcium transients in the activity-dependent case, it is first necessary to understand them in the absence of neurons- designated "spontaneous" calcium transients. These transients must rely solely on channels acting in the absence of neurotransmitters like glutamate and ATP.

Rui et al. (2020) suggests the importance of various factors on the integrity of these transients, depicted in Figure 2. Indeed, the authors show that the transients rely on some

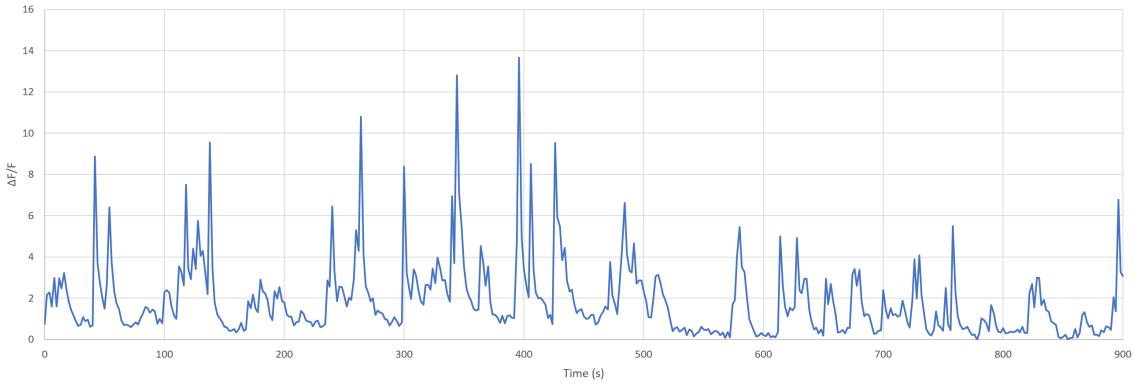

Figure 2: Data recorded by Rui et al. 2020 from a given region of interest, (ROI) of length ~ 20 μm on a branch of a complex OPC. The change in fluorescence, $\frac{\Delta F}{F}$, from fluorescent dye Fluo-4 is used to determine the relative change in calcium concentration over time [18].

external calcium flux through the cell membrane, as putting cells in a calcium-free buffer removes oscillations all together.

Finally, the nature of these transients varies throughout the development of the OL lineage. Through OL development, cells begin as oligodendrocyte progenitor (OPC) bipolar cells, with two large protrusions from the cell soma, then develop a simple structure, with some limited branching in the arm structure. These cells then form a complex actin cytoskeleton with a large degree of branching and, finally, become myelinating when they are able to produce MBP. In bipolar cells, transients are low amplitude and infrequent. As the cell grows, transients become more frequent and higher amplitude until the cell reaches the complex OPC stage. Finally, once the cell begins to produce myelin, transients become much less frequent and lower amplitude once again. Evidence suggests that, at this stage, many of these transients become localized to the myelin sheath itself [18].

Additionally, Bassetti et al. (2020) argue the transients depend on calcium flux through ryanodine receptors on the endoplasmic reticulum (ER) membrane as inhibiting them with ryanodine results in oscillations that are purely sub-threshold [2]. They also make a case for the role of the sodium calcium exchanger, although the source of depolarization resulting in significant flux through this channel is unknown.

While these factors have recently become elucidated, other potential contingencies of these transients remain unknown.

1.4 Modelling calcium

Calcium dynamics is a vast field with enormous variations in the way computational models are constructed. One of the simplest and best studied models was proposed by Li and Rinzel in 1994. According to this model, calcium concentration in the cytosol C and the open fracion of IP3Rs h are described by

$$\frac{dC}{dt} = J_{IP3} - J_{SERCA} + J_{LEAK}, \tag{1}$$

$$\frac{dh}{dt} = a_h(1-h) - b_h h, \tag{2}$$

where the activation rate a_h and deactivation rate b_h of IP3 receptors are given by

$$a_h = a_2 d_2 \frac{IP3 + d_1}{IP3 + d_3} \text{ and } b_h = a_2 C. \tag{3}$$

The IP3R flux J_{IP3} is given by

$$J_{IP3} = c_1 v_1 (\frac{IP3}{IP3 + d_1})^3 (\frac{C}{C + d_5})^3 h^3 (C - C_{ER}), \tag{4}$$

which closely follows a Hodgkin-Huxley-like flux with open probability determined by cytosolic calcium, IP3 concentration, and a time dependent term h multiplying the calcium gradient. The SERCA pump flux into the ER and leak across the ER membrane are described by

$$J_{SERCA} = \frac{v_3 C^2}{k_3^2 + C^2} \text{ and } J_{LEAK} = c_1 v_2 (C - C_{ER}), \tag{5}$$

a second-order Hill function in cytosolic calcium and linear term multiplying the gradient respectively. Finally, in this model, calcium is conserved intracellularly and, thus, ER calcium concentration is given by

$$C_{ER} = \frac{(c_0 - C)}{c_1}. \tag{6}$$

This model is a classic slow-fast oscillator with a linear-like nullcline intersecting a cubic-like nullcline. The dynamics of the model depend wholly on the location of intersection of these nullclines. An intersection in the left branch is a low but excitable steady state (a

stable focus) representing insufficient cytosolic calcium levels/IP3 concentration for calcium-induced-calcium-release to take place at the ER. When the intersection occurs in the middle branch of the cubic nullcline, the system crosses a Hopf bifurcation into a stable limit cycle where cytosolic calcium is oscillatory. Finally, an intersection at the right branch of the cubic nullcline describes where cytosolic calcium concentrations are too high for sustainable oscillations, a state that is usually cytotoxic [11].

2 Methods

2.1 Stochasticity

2.1.1 Measuring stochasticity

A method proposed by Sneyd et al. 2016 to quantify the level of irregularity in a signal and its cause involves plotting the average inter-spike interval and its standard deviation of a calcium time-series collected from many cells. Snyed reasons in this analysis that in a culture of cells with a heterogeneous characteristics will produce calcium time-series with different average period and standard deviation. Nonetheless, an unchanging mechanism for the generation of spikes should produce a relationship between these points. As such, from this relationship, we can draw conclusions about the nature of this mechanism. Sneyd posits that the expected relationship between the standard deviation σ of oscillations and the average period T_{avg} should roughly follow the the linear equation

$$\sigma = \alpha(T_{avg} - T_{min}) + \sigma_{min}, \tag{7}$$

where α is the coefficient of variation, T_{min} is the lowest average period observed and σ_{min} is the lowest standard deviation measured.

The parameter α indicates how the degree of irregularity between transients changes as their average period changes. In the case that $\alpha = 0$, the level of irregularity is constant irrespective of the length between spikes (if $\sigma = 0$ here, the spikes are always perfectly regular). Conversely, when $\alpha = 1$, transients can vary nearly and much as their average period, potentially within some absolute refractory period. In this case, transients can be well represented by a pure Poisson process. Sneyd argues that a strong linear relationship

between σ and T_{avg} is robust to variations in many parameters. Such a relationship, he concludes, can only be produced by purely stochastic spike generation since no other mechanism (eg. a perturbed system in its oscillatory regime) would yield such a well defined relationship [19].

In this analysis, a Python script is used to pick-peaks in the data and simulation. Linear fitting is used to extract parameters.

2.1.2 Explaining stochasticity

Calcium induced calcium release happens on a spatially hierarchical structure. Single channels are fundamentally stochastic and open and close on the order of μs to ms. Channels form clusters that release calcium when channels flux synchonously, with some level of cooperativity. Entire clusters typically flux calcium on the order of 10s to 100s of ms. Finally, when clusters, usually about 5-7 μm apart, release calcium synchronously, a cell wide calcium transient occurs. This requirement for synchrony of many random events on a hierarchical scale is expected to produce the irregularity observed [19].

2.2 Modifying the Li-Rinzel model

Incorporating stochasticity into the model, to mimic the role of a spatial hierarchy, we modify Equation 2

$$\frac{dh}{dt} = a_h(1-h) - b_h h + \sigma\zeta, \tag{8}$$

where $\zeta \sim \mathcal{N}(\mu = 0, \sigma^2 = 1)$ is a normally distributed random variable and σ is its standard deviation. Equation 8 is a stochastic differential equation drifting about the expected value for h as previously described. This model is constructed so that in the absence of noise, it sits at the low steady state, a stable focus, and a sufficiently large noise-induced perturbation will lead to a large excursion from steady state, producing a calcium transient. The parameter σ can be adjusted to control the proportion of these perturbations that induce a transient to those that are simply sub-threshold.

Additionally, in oligodendrocytes, calcium is clearly not conserved intracellularly and plays a significant role in model dynamics. Thus, we can rewrite Equations 1 and 6 as

$$\frac{dC}{dt} = J_{ER} + J_{IN} - k_{out}C, \tag{9}$$

$$\frac{dC_{ER}}{dt} = -\gamma J_{ER}, \tag{10}$$

where the term $k_{out}C$ represents calcium exocytosis, γ encapsulates the ratio volume in the ER to the cytosol, and the flux through the ER membrane J_{ER} is given by

$$J_{ER} = J_{IP3} + J_{RYR} + J_{LEAK} - J_{SERCA}. \tag{11}$$

The contribution of the ryanodine receptors J_{RYR} can be modelled by the third-order Hill function in cytosolic calcium multiplying the intermembrane gradient

$$J_{RYR} = \frac{v_r C^3}{C^3 + k_r^3}(C - C_{ER}). \tag{12}$$

The inward flux

$$J_{IN} = v_{in} + v_{tdep}, \tag{13}$$

can be broken into its static and dynamic quantities, v_{in} and v_{tdep} respectively. The time-dependent quantity v_{tdep} is largely phenomenological since the precise dependence of the inward flux on cytosolic calcium is unknown and it's main purpose is to attenuate a given transient to match signal shape observed in the data. The model is dynamically sufficient in its absence. This quantity is given by

$$\frac{dv_{tdep}}{dt} = \frac{v_\infty - v_{tdep}}{\tau_{tdep}} \text{ for } v_\infty = v_{max}C. \tag{14}$$

Here, the inward flux lags cytosolic calcium by time constant τ_{tdep}.

2.3 Spatial calcium transients

2.3.1 A reinforcement mechanism

Finally, these transients are fundamentally spatial. A simple Gillespie simulation [7] shows calcium diffusion is not sufficient for the rate of calcium flow in oligodendrocyte branches and relative change in concentration cannot be simply explained by diffusion [8]. We thus

propose a reinforcement mechanism whereby a transient at one location along an oligodendrocyte branch will diffuse to an adjacent site along the ER membrane, initiating a transient at each adjacent site by calcium induced calcium release [19]. As such, we expect each random perturbation to initiate a local bidirectional transient in the branching structure. Hence, we modify Equation 9

$$\frac{\partial C}{\partial t} = D_c \frac{\partial^2 C}{\partial x^2} + J_{ER} + J_{IN} - k_{out} C, \tag{15}$$

where D_c is the diffusion coefficient of buffered calcium.

2.3.2 Solving PDEs on a graph

There is a reason to believe that the branching structure of oligodendrocytes is linked to the nature of these transients. As demonstrated by Rui et al. 2020, the transients become larger and more frequent as the total length and connectivity of branches in an OL lineage cell increase. To investigate this, general purpose software was written to solve systems of n coupled equations of the form

$$\frac{\partial y_i}{\partial t} = f_i(t, y_j, \frac{\partial y_j}{\partial x}, \frac{\partial^2 y_j}{\partial x^2}) \text{ for } i = 1, 2, ..., n \text{ and any } j \text{ in } \{1, 2, ..., n\}, \tag{16}$$

along the edges of an arbitrary graph.

In 1D Euclidean space, a variable y (continuous in space) can be discretized into N compartments. The following second derivative matrix G can be constructed by finite differences

$$\vec{y}\,'' = (\Delta x)^{-2} G \vec{y} = (\Delta x)^{-2} \begin{bmatrix} 1 & -2 & 1 & 0 & \dots & 0 & 0 & 0 \\ 0 & 1 & -2 & 1 & \dots & 0 & 0 & 0 \\ 0 & 0 & 1 & -2 & \dots & 0 & 0 & 0 \\ \vdots & \vdots & \vdots & \vdots & \ddots & \vdots & \vdots & \vdots \\ 0 & 0 & 0 & 0 & \dots & 1 & -2 & 1 \end{bmatrix} \begin{bmatrix} y_1 \\ y_2 \\ y_3 \\ \vdots \\ y_N \end{bmatrix}. \tag{17}$$

In a graph, however, diffusion at a compartment with more than two outward edges is expected to have a greater diffusive flux than a compartment along an edge (ie. only two directions for a particle to diffuse). Specifically, if equations are to be solved at the vertices with edges describing proximity, one would expect the elements

$$G_{ij} = \begin{cases} 1 & \text{for } i \sim j \\ -d_{ij} & \text{for } i = j \\ 0 & otherwise \end{cases}, \tag{18}$$

where $i \sim j$ denotes two vertices i and j are connected by an edge and d_{ij} is the degree of the i^{th} vertex, ie. the number of edges it touches.

When solving equations along edges with defined length, one needs to split an edge into compartments of size Δx, equivalently define each compartment as a vertex in a far larger graph, and then compute the second derivative matrix by Equation 18. However, to minimize space and time complexity, one can generate G by realizing many of the compartments will be adjacent to only two others, ie. fall in the middle of an edge, and thus G will look very much like in the 1D Euclidean case (Equation 17). A simplified outline of an original iterative algorithm for computing G is given below.

Algorithm 1 Second derivative matrix of graph

```
0: procedure DISCRETIZE(num_comparts)
0:   initialize G as in 1D Euclidean case
0:   number compartments
0:   compute a cumulative sum of compartment number at nodes
0:   for each vertex do
0:     cut default connections
0:     assign junction according to a set convention
0:     edit G according to adjacency/degree
0:   end for
```

Graph code is made as an open-source (Python) and complied into a reusable package for solving ubiquitous PDEs on arbitrary graph structures. It is available at `https://github.com/kushasareen/oligo`.

3 Results

3.1 Stochasticity

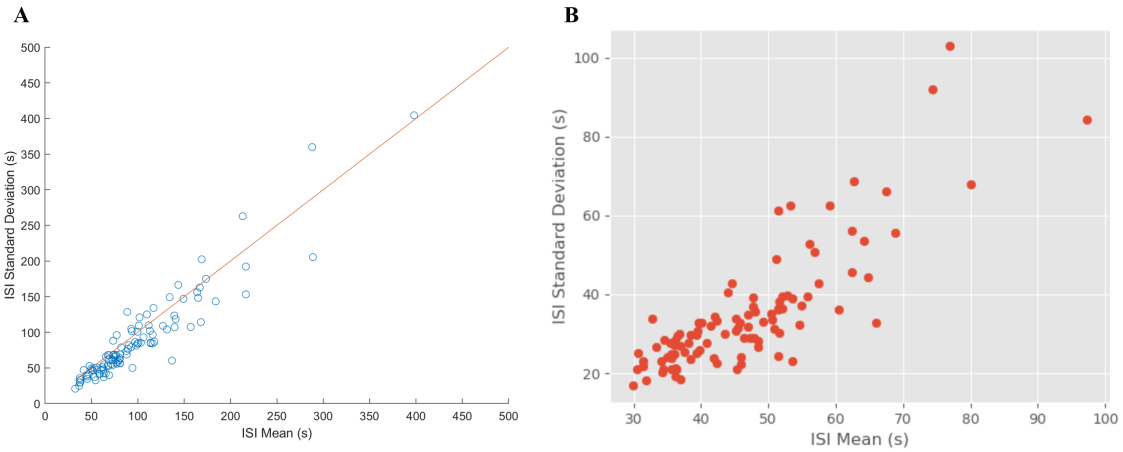

Figure 3: $T_{avg} - \sigma$ plot of the experimental data (A) and simulation (B) are shown. Notice the similarity between the two and random nature of both.

To determine if the transient spike in calcium data and simulation are purely stochastic, we used Eq. (7) to quatify the relation between the standard deviation (σ) of the oscillations and the average interspike interval (ISI) as suggested by Sneyd et al 2016 [19]. Figure 3 shows that both the simulations and the data exhibit a slope near 1, and an absolute refractory period that is comparable. The relatively large slope implies the calcium transients are mostly random, an outcome similar to that seen in other glial cells [19].

3.2 Graph diffusion

Figure 4 depicts a proof of concept for the graph PDE solver by simulating diffusion. Particles are initialized on the middle of the branch from vertex 1 to 2. Notice a greater concentration of particles is found near vertex 2 than vertex 1 since particles have fewer directions to diffuse, a phenomenon not directly observed in simple linear diffusion. This solver is used for model simulations on a single edge to minimize complication, although future experiments could elucidate the role of oligodendrocyte structure on calcium transients.

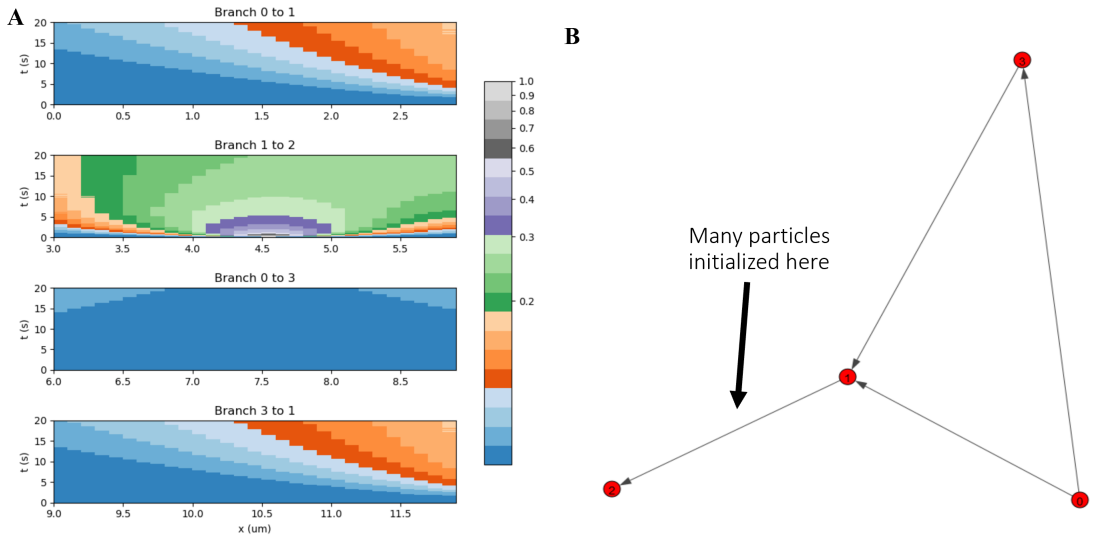

Figure 4: A proof-of-concept of an original graph PDE solver. Many particles are initialized on the edge from vertex 1 to 2 on an arbitrary graph structure (B). (A) shows the evolution of these particles in time along each branch. A diffusion coefficient of 1 $\frac{\mu m^2}{s}$ is used and concentrations are below 1 M. When particles cross a vertex on (B), they begin to appear on different branch on (A).

3.3 Model output

Figure 5 portrays a sample time-series simulation produced by the model. The evolution in time of dynamic variables of the model is shown. The first panel shows cytosolic calcium concentration over time. This matches what is seen experimentally, in that spikes are irregular and the slope of the upstroke is similar. The slope of the downstroke is, however, far quicker than that seen in the data. The second panel shows the time-dependent inward flux, lagging cytosolic calcium transients induced by calcium flux from the ER. Panel 3 shows the fraction of open IP3 receptors. This fraction is noisy and variable but not necessarily in phase with the calcium transients. Finally, the last panel shows the ER calcium concentration, in phase with cyctosolic calcium, resulting in a prototypical sawtooth pattern.

This model is dynamically very similar to the Li-Rinzel model. Both the IP3 concentration and inward membrane calcium flux contribute to sustainable cytosolic calcium levels. As such, increasing either of these parameters in the absence of noise will move the model

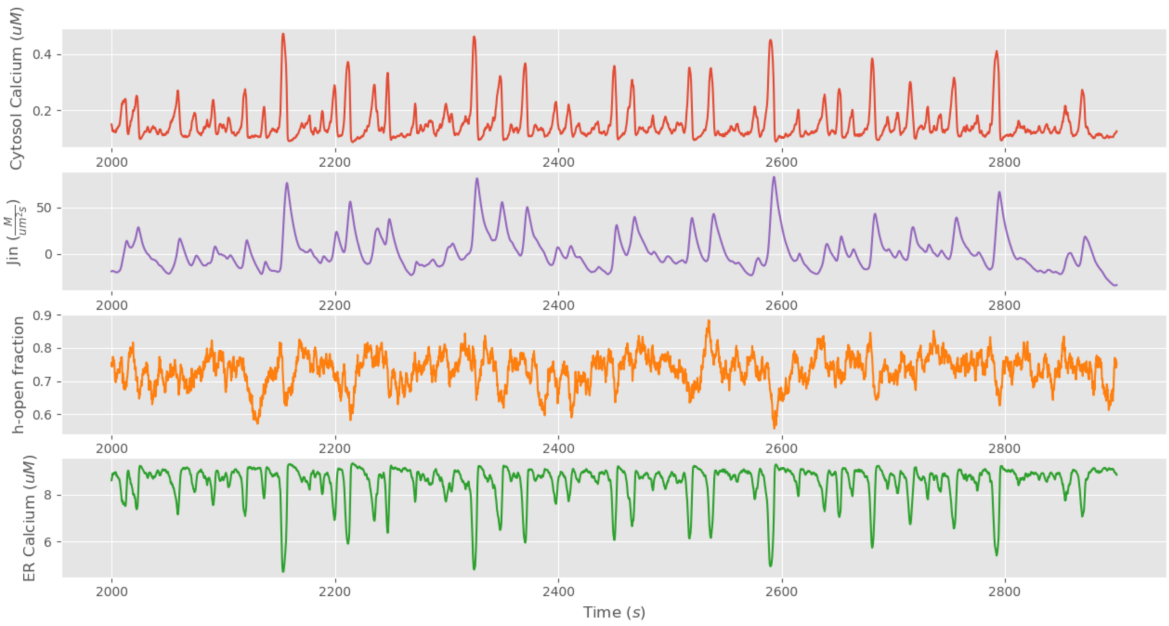

Figure 5: A sample time course simulation of the model over 900 seconds. From bottom to top, the panels show cytosolic calcium concentration, time-dependent inward flux, open-fraction of IP3 receptors and ER calcium concentration.

through the three regimes defined by the branches of the cubic nullcline. Additionally, when noise is present, increasing inward membrane flux brings the model closer to the oscillatory regime. As a result, smaller perturbations are able to initiate a transient which in turn causes the average frequency of transients to increase.

Figure 6 illustrates a meshgrid of calcium transients in space and in time. On average, transients travel 15-20 μm along and edge. This is in line with what is seen experimentally.

Since the model spikes are driven by a large excursion from a stable focus, the model is not excitable during a transient, implying a small absolute refractory period. Notice, for instance, what happened at x = 35 μm and t = 2020 s in Figure 6. Here, two waves initiate at neighbouring points and travel to x = 35 μm at a later time. These waves collide and annihilate, neither continuing to travel along its previous trajectory.

3.4 Dynamics

Figure 7 depicts the nullclines of the 3D system. For visualization, the time-dependent inward flux is omitted as it is the least influential on model dynamics. As in the 2D case, a

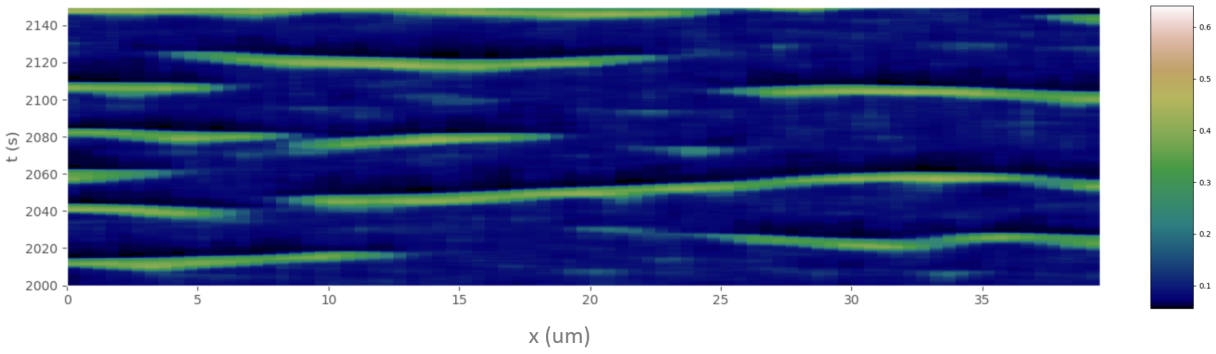

Figure 6: A meshgrid of cytosolic calcium concentration along a 40 μm branch over 150 seconds. Stochastically generated travelling waves are shown to travel in both directions along the branch.

noise-induced perturbation leads to a large deviation from the stable steady-state. Indeed, this model is simply an expansion of the 2D case, accounting for flux through the cell membrane [11].

Figure 8 demonstrates the dependence of the transients on inward flux, flux through ryanodine receptors, and SERCA pumping replenishing the ER calcium stores. Experimental analogs from the literature are included for comparison. Maintaining these relationships ensures model robustness and the integrity of any model predictions.

4 Discussion

4.1 Implications

The reduced spatial scale in the oligodendrocyte arm amplifies the role of noise in the production of transients. This trend is seen in other cells with similar branching structure like astrocytes and microglia.

The time dependent inward flux v_{tdep} represents a cooperative inward calcium flux that lags cytosolic calcium by approximately 15 seconds. There are a number of potential physiological sources for such a flux. It has been speculated that membrane volatage in oligodendrocytes is highly variable. In fact, Berret et al. 2017 shows that oligodendrocytes are excitable cells, though the source of depolarizations in an oligodendrocyte-only culture

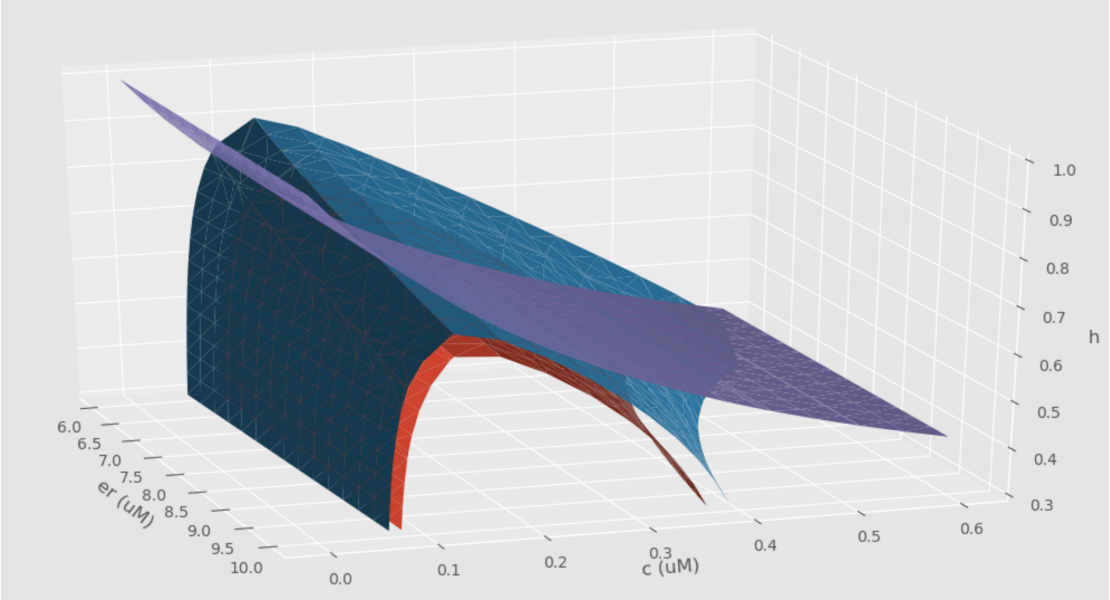

Figure 7: 3D nullclines for a simplified model, analogous to well-studied 2D case. The model is at steady state at the intersection the 3 manifolds near $C = 0.1$ μM, $h = 0.7$ and $C_{ER} = 8.0$ μM. A noise-induced perturbation results in large excursion before returning to steady state.

remains unclear [3]. It's possible some local depolarization following a transient could result in increased inward flux through voltage gated calcium channels. Additionally, stretch-activated calcium channels could potentially lead to local osmotic stress during an ER initiated transient, resulting in increased flux through the cell membrane. Finally, calcium could simply act as an agonist for a different membrane receptor, producing a calcium influx that follows a transient.

Travelling waves in models of excitable media are a common occurrence. For example, Oprea et al. 2020 explores spatiotemporal waves in the cortex, similar to those observed in animal models as well as humans [15]. In our model, a wave initiated at a given point will diffuse to its neighbourhood, moving the nullcline intersection closer to the middle branch, thus making the region far more excitable. It is believed travelling waves in the OL structure, much like those in the cortex, convey information between regions that are spatially separated. Its believed this information could be a cue for MBP transcription, involving calmodulin, in the cell soma initiated by signals at the distal OL processes. Alternatively,

a general increase transient frequency due to increased calcium conductivity could result in the increased rate of growth of the actin cytoskeleton, a process known to involve calcium.

This type of model is highly plastic and generalizable. For instance, when a full model of spontaneous calcium transients is fully developed, the activity-dependent component is easy to implement by simply introducing a boundary condition for compartments with degree only 1.

4.2 Shortcomings

Techniques for numerically fitting systems of partial stochastic differential equations are not currently computationally feasible. Indeed, finding a set of parameters that produces simulations that visually match the data is a difficult task. Different parameter sets produce a large variation in the qualitative output of the model. Particularly, a parameter set where the downstroke of a simulated transient matches that of a transient observed experimentally was difficult to find.

Additionally, it remains to be seen exactly which sources of membrane flux are important. The v_{tdep} term in the model suggests some cooperative inward calcium flux with a time constant near 15 seconds. Whether other membrane fluxes are significant and the particular role they play, however, is an experimental problem that cannot be solved by purely theoretical work.

Furthermore, the significance of these stochastically produced spatial transients is brought into question. Previous literature has posited that these transients encode information in their patterns. However, since the transients seem to be generated stochastically, this seems unlikely. Many questions remain about the origin and function of these transients. Which particular signals are these transients meant to transmit in space? Is there a functional role of the stochasticity or is it purely a byproduct of the small spatial scale? What are the mechanisms by which they are implicated in OL maturation and myelin sheath growth?

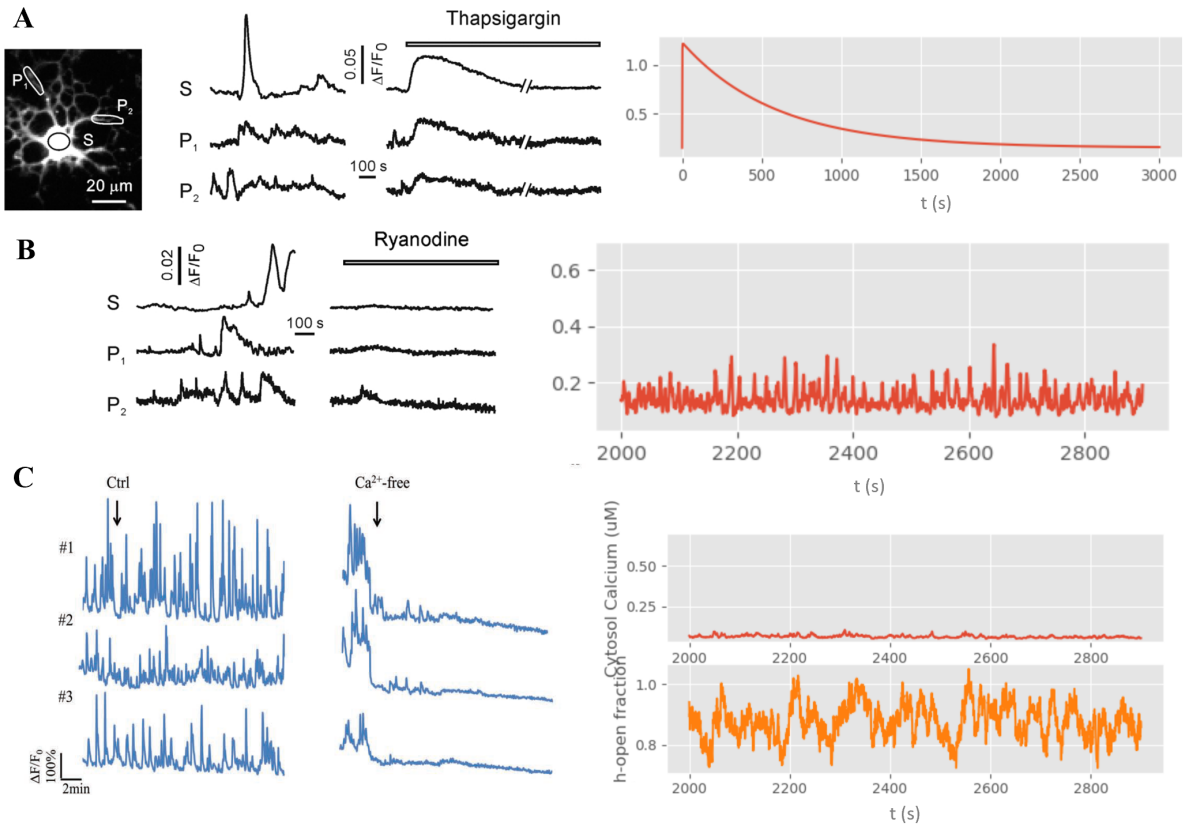

Figure 8: A comparison of empirical and simulated results when various flux are inhibited. (A) depicits the calcium trace when SERCA pumping, and hence the contribution of ER fluxes, is eliminated. Data from Bassetti et al. 2020 vs. simulation. (B) shows when ryanodine receptors are inhibited, simulated and from Bassetti et al. 2020 [2]. (C) demonstrates calcium transients depend on a positive inward flux through the cell membrane. Results from Rui et al. 2020 [18].

5 Conclusions

Recent evidence suggests the role of calcium dynamics in the regulation of activity-dependent myelination. A data-driven model for calcium transients in the oligodendrocyte lineage based on time-series $\Delta F/F$ calcium data shows spontaneous irregular transients. Transients appear to be stochastically-generated local travellings waves in the oligodendrocyte structure. Furthermore, modelling efforts show the frequency of these transients increases with the inward membrane flux of calcium, explaining the observation of fast transients

in the presence of high frequency neural activity. This supports a role for calcium in the maturation of the oligodendrocyte lineage, perhaps a regulator for the growth of the actin cytoskeleton or as a transcription/translation factor for MBP. We argue these transients must have an absolute refractory period and cannot encode information in their patterns.

The model can be improved by determining a parameter set that better qualitatively fits the profile of the experimental data. A clear future direction is to include activity-dependent channels in our modelling. This adjustment should allow for expansion of the model to predict how exactly myelin remodelling depends on neural activity.

Acknowledgements

The authors acknowledge the generous support from the Zheng Laboratory at Emory in their willingness to provide experimental data. Additionally, this project was funded in part by the McGill Initiative in Computational Medicine.

References

[1] M. Baraban, S. Koudelka, and D. Lyons. Ca 2+ activity signatures of myelin sheath formation and growth in vivo. *Nature Neuroscience*, 21:19–23, 2018.

[2] D. Bassetti, J. Hammann, H. Luhmann, R. White, and S. Kirischuk. Ryanodine receptor and sodium-calcium exchanger-mediated spontaneous calcium acivity in immature oligodendrocytes in culutres. *Neuroscience Letters*, 732:1–5, 2020.

[3] E. Berret, T. Barron, J. Xi, E. Debner, E. Kim, and J. Kim. Oligodendroglial excitability mediated by glutamatergic inputs and nav1.2 activation. *Nature Neuroscience*, 8:1–15, 2017.

[4] L. Cleemann and M. Morad. Role of ca2+ channel in cardiac excitation-contraction coupling in the rat: evidence from ca2+ transients and contraction. *Journal of Physiology*, 432:283-312, 1991.

[5] LM. De Biase, SH. Kang, and EG. Baxi. Role of ca2+ channel in cardiac excitation-

contraction coupling in the rat: evidence from ca2+ transients and contraction. *Journal of Neuroscience*, 35:12650-12662, 2011.

[6] RD. Fields and Y. Ni. Nonsynaptic communication through atp release from volume-activated anion channels in axons. *Sci Signal*, 3, 2010.

[7] D. Gillespie. Exact stochastic simulation of coupled chemical reactions. *Stochastic Simulation of Coupled Chemical Reactions*, page 2339-2361, 1977.

[8] D. Holcman and Z. Schuss. Diffusion laws in dendritic spines. *Journal of mathematical neuroscience*, 1:10, 2011.

[9] AM. Krasnow, MC. Ford, LE. Valdivia, SW. Wilson, and D. Attwell. Neurotransmitter receptors in the life and death of oligodendrocytes. *Nature Neuroscience*, 21:24–28, 2018.

[10] R. Káradóttir and D. Attwell. Neurotransmitter receptors in the life and death of oligodendrocytes. *Neuroscience*, 145:1426-1438, 2007.

[11] Y. Li and J. Rinzel. Equations for insp3 receptor-mediated [ca2+]i oscillations derived from a detailed kinetic model: a hodgkin-huxley like formalism. *Journal of Theoretical Biology*, 166, 1994.

[12] I. Lundgaard, A. Luzhynskaya, and JH. Stockley. Neuregulin and bdnf induce a switch to nmda receptor-dependent myelination by oligodendrocytes. *PLoS Biology*, 11:12, 2013.

[13] R. Miller. Calcium control of myelin sheath growth. *Nature Neuroscience*, 21:2–3, 2018.

[14] M. Monje. Myelin plasticity and nervous system function. *Annual Review of Neuroscience*, 41:61–76, 2018.

[15] L. Oprea, C. Pack, and A. Khadra. Machine classification of spatiotemporal patterns: automated parameter search in a rebounding spiking network. *Cognitive Neurodynamics*, 14:267–280, 2020.

[16] PM. Paez and DA. Lyons. Calcium signaling in the oligodendrocyte lineage: Regulators and consequences. *Annual Review of Neuroscience*, 7:169, 2020.

[17] J. Poledna. Mechanism of intracellular calcium transients. *General Physiological Biophysics*, 10:475-484, 1991.

[18] Y. Rui, S. Pollitt, K. Myers, Y. Feng, and J. Zheng. Spontaneous local calcium transients regulate oligodendrocyte development in culture through store operated calcium entry and release. *eNeuro*, 2020.

[19] J. Snyed, G. Dupont, M. Falcke, and V. Kirk. *Models of Calcium Signalling*. Springer, New York, NY, 1nd edition, 2016.

[20] GS Tomassy, DR Berger, and HH Chen. Distinct profiles of myelin distribution along single axons of pyramidal neurons in the neocortex. *Science*, pages 319–324, 2014.

[21] H. Wake, PR. Lee, and RD. Fields. Control of local protein synthesis and initial events in myelination by action potentials. *Science*, 333:1647-1651, 2001.